Frequency-Dependent Polarizability of Boron Nitride Nanotubes: A Theoretical Study

Jacob Kongsted,[†] Anders Osted,[†] Lasse Jensen,*[,‡] Per-Olof Åstrand,[†,§] and Kurt V. Mikkelsen[†]

Department of Chemistry, H. C. Ørsted Institute, University of Copenhagen, DK-2100 Copenhagen Ø, Denmark, Theoretical Chemistry, Material Science Center, Rijksuniversiteit Groningen, Nijenborgh 4, 9749 AG Groningen, The Netherlands, and Materials Research Department, Risø National Laboratory, DK-4000 Roskilde, Denmark

Received: June 6, 2001; In Final Form: July 21, 2001

In the present work, we have calculated the static and frequency-dependent polarizability tensors for a series of single-walled boron nitride nanotubes and compared them with corresponding results for carbon nanotubes. The calculations have been performed by employing a dipole−dipole interaction model based on classical electrostatics and an Unsöld dispersion formula. In comparison, we have carried out *ab intio* calculations at the SCF level of the static polarizability of the smaller nanotubes with the STO-3G basis set. For the frequency-dependent polarizability of C_{60}, we found excellent agreement among the most accurate SCF calculations in the literature, the interaction model, and experimental results. In particular, the frequency dependence is modeled accurately indicating that the interaction model is a useful tool for studying the frequency dependence of materials. For the nanotubes, we observe the same trends in the interaction model and in the SCF STO-3G results when the number of atoms is increased. However, the values obtained with the interaction model are about 100% larger than the corresponding SCF STO-3G results, due to the small size of the STO-3G basis set. We also find that the boron nitride nanotubes have smaller magnitudes of the polarizability tensor components than the corresponding components for the carbon nanotubes with the same geometry and number of atoms. Furthermore, we find that the geometry of the tube has a large influence on the anisotropy of the polarizability components, whereas the mean polarizability remains almost unaffected when the geometrical configuration is modified. Finally, we observe a relatively small frequency dependence of the polarizability tensor of BN nanotubes.

I. Introduction

Today, a large effort is put into improving the models of optical response properties at a molecular level because of its practical use in the construction of new optoelectronic and photonic devices. In particular, the prediction and understanding of (hyper)polarizabilities have received attention.[1−5] For example, conjugated organic compounds have been considered because of their delocalized π-electron systems along the chain axis.[3,4] In addition, other promising classes of carbon compounds such as fullerenes and carbon nanotubes (C-NTs) have been investigated.[6,7] Since the discovery of C-NTs[8] and in particular the single-walled C-NTs,[9,10] substantial interest has been devoted to predicting the optical response properties of these systems.[11−21]

C-NTs exist in various forms such as single or multiwalled, with various diameters, lengths, and intramolecular geometries, closed-ended (capped) and also with torus structures.[6,22] Both theory and experiments suggest that 4 Å is the smallest stable diameter for a C-NT,[23] which corresponds to, e.g., a [5,0]-nanotube. The roll-up vector [*m*,*n*] is used to characterize the nanotubes and defines its symmetry and diameter.[6] Armchair nanotubes correspond to roll-up vectors [*n*,*n*] and zigzag tubes to [*n*,0], respectively. Both armchair and zigzag nanotubes are achiral, in contrast to all other tubes, which are chiral. The linear and nonlinear optical response properties for fullerenes[24−31] and single-walled C-NTs[11−19] have been studied extensively by theoretical means. Response properties of the fullerenes C_{60} and C_{70} have also been studied in quite some detail experimentally.[32,25,33−40] However, only a few experimental studies of optical response properties of C-NTs have been reported.[20,21] The symmetry of carbon nanotubes has great influence on the (hyper)polarizability leading to larger values for armchair than for zigzag tubes with an equal number of atoms. Also, length, diameter, chirality, and number of caps are important in determining the (hyper)polarizability of the tubes.[11,14−18] In addition to the studies of pure carbon compounds, different kinds of impurities have been introduced into fullerenes and nanotubes. Substitution of carbon with boron and nitrogen have been carried out, producing boron-, nitrogen-, and boron−nitrogen-doped carbon nanotubes[41−49] and totally substituted boron nitride nanotubes (BN-NTs).[46,47,50−62] The structure of these new boron−nitrogen-containing fullerenes and nanotubes have been studied and compared with that of carbon nanotubes.[63−76] In particular, it has been noted that BN-NTs have an almost constant band gap of 5.5 eV with respect to the geometric configuration of the tube whereas the band gap of carbon nanotubes show a strong geometry dependence.[67]

The effects of doping C_{60}-based C-NTs[77] and the fullerene C_{60}[78,79] with boron and nitrogen on the second hyperpolarizability, γ, have been reported. These studies show that doping enlarges γ by several orders of magnitude compared to that of the pure fullerene and C-NTs, suggesting B-, N-, and BN-doped C-NTs as well as pure BN-NTs as serious candidates for photonic devices. However, to our knowledge, no studies of the polarizability of BN-NTs have been carried out so far.

* Corresponding author: E-mail: l.jensen@chem.rug.nl
[†] Ørsted Institute, University of Copenhagen.
[‡] Material Science Center, Rijksuniversiteit Groningen.
[§] Materials Research Department, Risø National Laboratory.

10.1021/jp0121724 CCC: $20.00
Published on Web 10/03/2001

In the present work, we therefore investigate the frequency-dependent polarizability tensor of several single-walled (SW) zigzag and armchair BN-NTs and compare with the corresponding C-NTs. A classical frequency-dependent dipole interaction model will be used,[80,81] which has been used previously to predict the frequency-dependent polarizability of carbon nanotubes.[18] We investigate the effect of variation in length, diameter and symmetry of the nanotubes on the dynamic polarizability.

II. Theoretical Background

Considering a set of N interacting atomic polarizabilities, the atomic induced dipole moment on atom p responding to an external electric field, E^{ext}, is given by[82]

$$\mu_{p,\alpha}^{\text{ind}} = \alpha_{p,\alpha\beta}(E_\beta^{\text{ext}} + \sum_{q\neq p}^{N} T_{pq,\beta\gamma}^{(2)} \mu_{q,\gamma}^{\text{ind}}) \tag{1}$$

where $T_{pq,\alpha\beta}^{(2)}$ is the so-called dipole interaction tensor

$$T_{pq,\alpha\beta}^{(2)} = \frac{3r_{pq,\alpha}r_{pq,\beta}}{r_{pq}^{5}} - \frac{\delta_{\alpha\beta}}{r_{pq}^{3}} \tag{2}$$

Following the Applequist approach,[82] the molecular polarizability can be written as

$$\alpha_{\alpha\beta}^{\text{mol}} = \sum_{p,q}^{N} B_{pq,\alpha\beta} \tag{3}$$

where **B** is the relay matrix defined in a super matrix notation as

$$\mathbf{B} = (\boldsymbol{\alpha}^{-1} - \mathbf{T}^{(2)})^{-1} \tag{4}$$

Since the electronic charge distribution is smeared out, the electric field at a nucleus will be damped by the charge distribution. This damping may be modeled by modifying the distance r_{pq} to obtain a scaled distance s_{pq}[81]

$$s_{pq} = \upsilon_{pq} r_{pq} = f(r_{pq}) \tag{5}$$

where υ_{pq} is a scaling factor and $f(r_{pq})$ is an appropriately chosen function of r_{pq}. Furthermore, if each component of r_{pq} also is scaled by υ_{pq}, the reduced distance becomes

$$s_{pq} = \sqrt{s_{pq,\alpha}s_{pq,\alpha}} = \upsilon_{pq}\sqrt{r_{pq,\alpha}r_{pq,\alpha}} = \upsilon_{pq} r_{pq} \tag{6}$$

which is consistent with the definition in eq 5. In eq 6, the Einstein summation convention for repeated indices has been employed. The damped interaction can thus be obtained by modifying only the interaction tensors

$$T_{pq,\alpha_1\ldots\alpha_n}^{(n)} = \nabla_{\alpha_1} \cdots \nabla_{\alpha_n}\left(\frac{1}{s_{pq}}\right) \tag{7}$$

which is equivalent to replacing r_{pq} by s_{pq} and $r_{pq,\alpha}$ by $s_{pq,\alpha}$ in the regular formulas for the interaction tensor. The form of the scaling function employed here is[81]

$$f(r_{pq}) = \sqrt{r_{pq}^{2} + \frac{\pi}{4a_{pq}}} \tag{8}$$

where a_{pq} is given by $a_{pq} = \Phi_p\Phi_q/(\Phi_p + \Phi_q)$. Φ_p is an atomic damping parameter. This particular form of the scaling function was obtained by approximating the interaction between two Gaussian charge distributions with exponents Φ_p and Φ_q.

Well below the first electronic absorption, the frequency dependence of the molecular polarizability is often approximated with an Unsöld-type of expression.[4] Here we assume that the atomic polarizability parameter has a similar frequency dependence[80]

$$\alpha_p(-\omega;\omega) = \alpha_p(0;0) \times \left[\frac{\overline{\omega_p}^2}{\overline{\omega_p}^2 - \omega^2}\right] \tag{9}$$

The atomic parameters α_p, Φ_p, and $\overline{\omega_p}$ have been fitted previously to the full tensors of quantum-mechanically computed molecular polarizabilities of a series of aliphatic and aromatic molecules containing the elements B, C, H, N, O, F, and Cl.[81] A more detailed description of the model used and the parametrization of the model parameters can be found in ref 81. The interaction model is not reparametrized in this work but adopted with the parameter values reported previously.

III. Computational Methods

The static polarizability tensor has been calculated for six series of BN nanotubes at the SCF level using the minimal STO-3G basis and the Gaussian 98 program package.[83] The two first series of nanotubes are armchair [6,6] BN-NTs containing from 48 to 144 atoms and [6,6] BN-NTs with hydrogen atoms attached to the ends (BN(H)-NTs) containing from 48 to 228 boron and nitrogen atoms. Also, a number of zigzag [9,0] BN-NTs, some with hydrogen atoms at the ends, were constructed. The geometries of these tubes were optimized using the Sybyl force field.[84] Two additional series of calculations were performed on nanotubes containing up to 200 atoms. The series of armchair BN-NTs with constant length was varied in diameter from a [5,5] to a [10,10] configuration. The zigzag structure, also with constant length, was varied from a [9,0] to a [18,0] configuration. These latter structures were constructed from C-NTs taken from ref 85 by substitution of carbon with boron and nitrogen atoms. No geometry optimizations were performed on these structures.

Because of the different levels of geometry optimization employed, an investigation was performed of the dependence of the polarizability on the geometry. A [6,6] armchair BN-tube containing 108 atoms was optimized using the Sybyl force field and at the PM3 level using the Gaussian 94 program package.[86] The diameter of the tube was calculated to 8.40 Å and its length to 10.32 Å at the PM3 level, and the optimization using the Sybyl force field resulted in a diameter of 8.09 Å and a length of 9.75 Å, respectively. When examining a borazine fragment in one of the nanotubes, we find that the geometry has changed considerably from that of borazine itself. By performing a geometry optimization of borazine at the PM3 level, we obtained the following geometry: d(B,N) = 1.44 Å, $\angle$(N,B,N) = 124.2°, and $\angle$(B,N,B) = 115.8°. For the BN tubes optimized at the PM3 level, we found that d(B,N) varies between 1.47 and 1.48 Å, $\angle$(N,B,N) varies between 118.7° and 119.8°, and $\angle$(B,N,B) is within the interval from 117.3° to 118.9° for the different kinds of segments in the tube. The obtained structure from the Sybyl force field optimization yields a d(B,N) that varies from 1.39 to 1.40 Å, an angle $\angle$(N,B,N) between 116.6° and 124.1°, and an $\angle$(B,N,B) between 116.9° and 124.1°.

A comparison of the static polarizability of a [6,6]BN-NT at three different levels of optimization (none, Sybyl force field, PM3) was carried out in order to investigate the effect of the small geometry differences. These calculations showed that the largest effects on the polarizabilities were around 3% both for

TABLE 1: Mean Polarizability, Anisotropy, and Polarizability Tensor Components of Benzene and Borazine (in au)

	$\bar{\alpha}$	λ	$\alpha_{\|\|}$	$\alpha_{\perp}$	ref
experimental					
benzene	69.63				89
borazine	54				89
theoretical					
SCF Sadlej					
benzene	69.50	29.24	45.21	80.97	29
borazine	56.09	17.83	41.52	63.38	90
this work					
SCF Sadlej[91]					
benzene	68.42	28.13	45.49	79.89	
borazine	57.39	22.91	42.12	65.03	
SCF STO-3G					
benzene	32.71	32.87	5.93	46.10	
borazine	26.91	24.25	7.11	36.81	
IM					
benzene	63.60	31.66	42.50	74.16	
borazine	55.74	23.82	39.86	63.68	

the QM and the IM calculations, which is in agreement with previous investigations.[18,27]

The IM parameters are in au: $\alpha_H = 1.280$, $\alpha_C = 8.465$, $\alpha_B = 8.649$, $\alpha_N = 6.169$, $\Phi_H = 0.358$, $\Phi_C = 0.124$, $\Phi_B = 0.074$, $\Phi_N = 0.268$, $\bar{\omega}_C = 0.447$, $\bar{\omega}_B = 0.467$, $\bar{\omega}_N = 0.649$, and they are all taken from ref 81. The frequency-dependent calculations were restricted to molecules containing the elements C, N, and B, but the parameter describing the frequency-dependence for the element H can be found in ref 81.

IV. Results

For the molecules and nanotubes investigated in this work, the mean polarizability $\bar{\alpha}$ can be written as

$$\bar{\alpha} = \frac{1}{3}[\alpha_{xx} + \alpha_{yy} + \alpha_{zz}] = \frac{1}{3}[2\alpha_{\perp} + \alpha_{||}] \qquad (10)$$

where the molecules or nanotubes have been oriented in such a way that $\alpha_{xx} = \alpha_{yy} = \alpha_{\perp}$ and $\alpha_{zz} = \alpha_{||}$. The anisotropy, λ, may be defined as

$$\lambda = \sqrt{(\alpha_{xx} - \bar{\alpha})^2 + (\alpha_{yy} - \bar{\alpha})^2 + (\alpha_{zz} - \bar{\alpha})^2}$$
$$= \sqrt{2(\alpha_{\perp} - \bar{\alpha})^2 + (\alpha_{||} - \bar{\alpha})^2} \qquad (11)$$

A. Polarizability Tensor of Benzene, Borazine, and C_{60}. In Table 1, we compare the mean polarizability, anisotropy, and polarizability tensor components of benzene and borazine. The results in Table 1 show good agreement between experimental and theoretical polarizabilities for both benzene and borazine, even though the SCF STO-3G method underestimate the polarizability considerably. We observe that the anisotropy decreases when improving the basis set.[87] It is also observed that, apart from the calculation using a STO-3G basis set, the tensor components for benzene are larger than the corresponding tensor components for borazine, which trivially leads to that also the mean static polarizability is higher for benzene than for borazine. This is expected since the degree of delocalization of the electrons is higher in benzene than in borazine. In addition, from a simple additive perspective, the polarizability is smaller for borazine than for benzene mainly because of that α_N is smaller than α_C.

Table 2 presents both theoretical and experimental results for the frequency-dependent mean polarizability of C_{60}. Recently, frequency-dependent linear response calculations of the polarizability of C_{60} using a Hartree−Fock reference wave function yielded a polarizability of 75.1 Å^3,[30] which is in good agreement with the experimental static polarizability of 76.5 ± 8 Å^3. [39] Also, the experimental frequency-dependent polarizability of 79.4 ± 4 Å^3[40] is in good agreement with the theoretical result of 76.4 Å^3.[30] However, due to the large experimental uncertainty, no definite conclusion can be drawn based on experiments concerning the dispersion of the polarizability of C_{60}. From Table 2, it is seen that the IM results of 77.5 Å^3 for the static polarizability and 78.2 Å^3 for the frequency-dependent polarizability are in excellent agreement with both the SCF results and the experimental values, and they also provide the same trends as the SCF calculations with respect to the frequency dependence. This indicates that our model is able to predict the polarizability of molecules larger than the ones included in the training set in ref 81.

TABLE 2: Static and Frequency-Dependent Isotropic Polarizability of C_{60} (Å^3) at $\omega = 0.0428$ au

method	$\bar{\alpha}(0)$	$\bar{\alpha}(\omega)$	ref
experimental	76.5 ± 8	−	39
experimental	−	79 ± 4	40
SCF 6-31++G	75.1	76.4	30
IM	77.5	78.2	this work

B. Dependence of the Polarizability on the Diameter of BN Tubes. In Figure 1a,b, we present a comparison of the static polarizability components of different armchair BN-NTs calculated at the SCF level with the STO-3G basis set and the interaction model. The Figures display the polarizability of the tubes as a function of the total number of B and N atoms. The tubes maintain the same length (9.84 Å) but vary in diameter from a [5,5]-NT to a [10,10]-NT. In Figure 1a, the polarizability along the tube ($\alpha_{||}$) is displayed, and Figure 1b presents the polarizability perpendicular to the tube ($\alpha_{\perp}$), respectively. It is found that the two methods predict the same trends. However, the polarizability component along the tube calculated at the SCF level is lower than the corresponding IM results, which is consistent with the results for benzene and borazine presented in Table 1. The relative increase in the polarizability component along the tubes is about 92%for the IM model and 49% at the SCF level if the number of B and N atoms is increased from 100 to 200. For the polarizability component perpendicular to the tubes, we obtain an increase of 135% in the IM model and 146% at the SCF level. Thus, in this case, the polarizability component increases most in the direction along the tubes. It is also noted that a simple additive model of the molecular polarizability does not describe the dependence of the polarizability on the diameter of the tube.

C. Dependence of the Polarizability on the Length of Carbon and BN Tubes. Figure 2a,b displays the polarizability components of [5,5]-C-NTs, [6,6]-BN-NTs and [6,6]-BN(H)-NTs as a function of the number of atoms heavier than hydrogen. The polarizability component along the tube is presented in Figure 2a, and the component perpendicular to the tube is presented in Figure 2b. The nanotubes maintain a constant diameter (7.07 Å for C-NT and 8.07 Å for BN-NT) but vary instead in length. From Figure 2a,b, it is clear that the polarizability increases in a nonlinear way as the number of atoms increases. Therefore, $\alpha_{||}$ and $\alpha_{\perp}$ cannot be described by an additive model as found also elsewhere for large conjugated systems.[88] In Figure 2a,b, it is seen that the largest relative increase in the polarizability component is along the tubes. Thus, the same trend is observed as that in Figure 1a,b, where the diameter was varied. It is also noted that attaching hydrogen atoms to the end of the tubes raises the polarizability in the IM

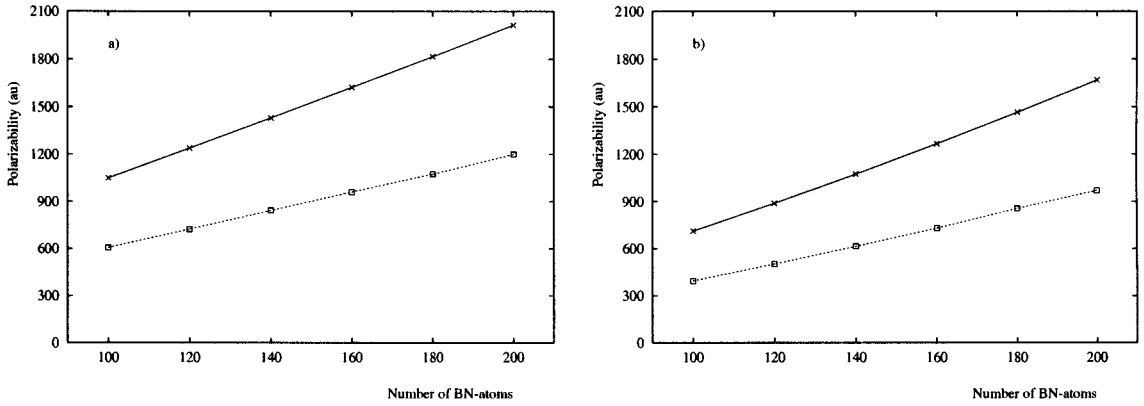

Figure 1. Static polarizability of the [5,5]-[10,10] BN-NTs as a function of the number of atoms. IM (—, ×) and SCF STO-3G (− −, □). (a) $\alpha_{\parallel}$ and (b) $\alpha_{\perp}$.

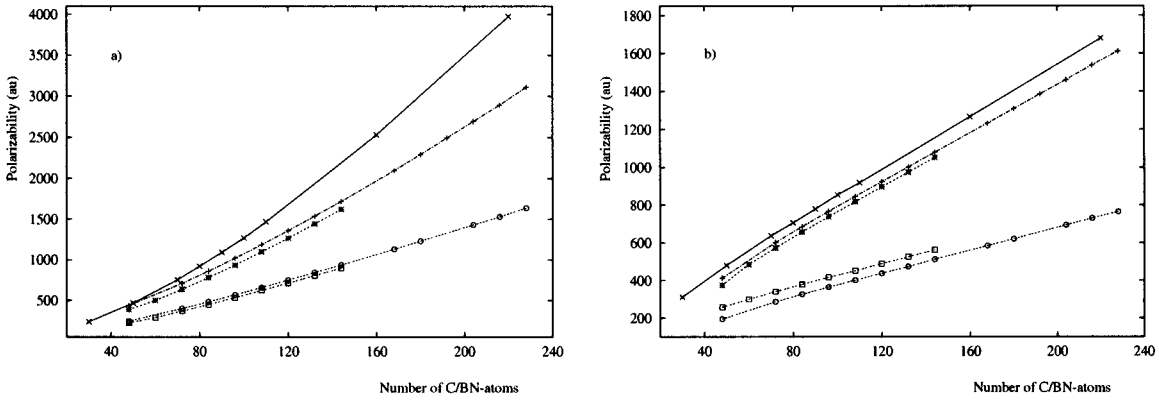

Figure 2. Comparison of the static polarizability of [5,5] C-NTs and [6,6] BN-NTs. IM [5,5]C-NT (—, ×), IM [6,6]BN(H)-NT (− · −, +), IM [6,6]BN-NT (···, *), QM [6,6]BN(H)-NT (···· ····, ○), and QM [6,6]BN-NT (·· ··, □). (a) $\alpha_{\parallel}$ and (b) $\alpha_{\perp}$.

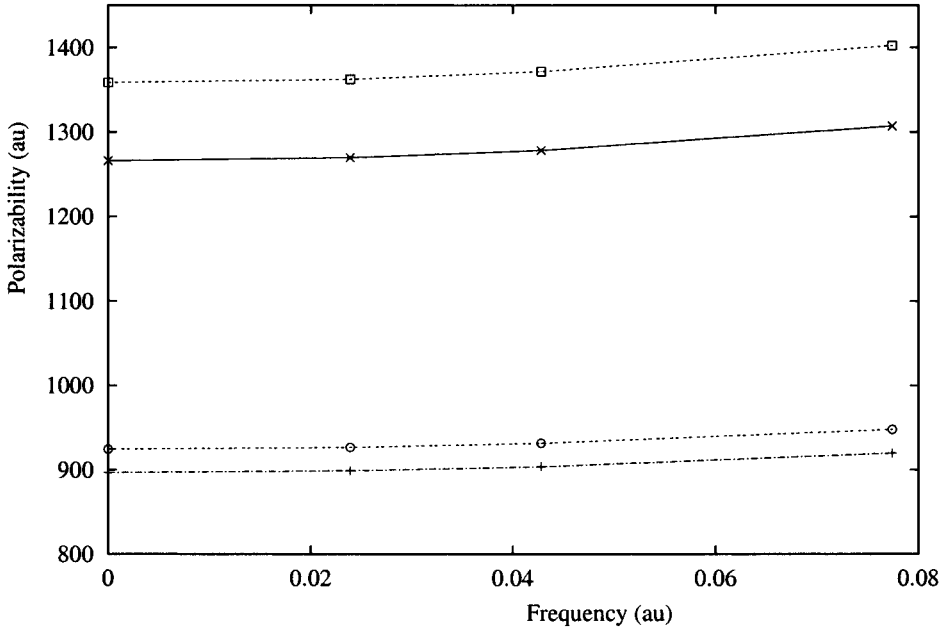

Figure 3. Frequency-dependent polarizability of the [6,6]BN-NT with 120 B + N atoms, calculated using IM with $\overline{\omega_B} = 0.4670$ au and $\overline{\omega_N} = 0.6490$ au. $\alpha_{\parallel}$ [6,6]BN(H)-NT (---, □), $\alpha_{\parallel}$ [6,6]BN-NT (—, ×), $\alpha_{\perp}$ [6,6]BN(H)-NT (− − −, ○), and $\alpha_{\perp}$ [6,6]BN-NT (− · −, +).

approach, while the polarizability is lowered in the SCF approach. The increase in the polarizability when adding hydrogen atoms to the ends is expected simply from an additive point of view. Since this is not observed for the SCF results, it is concluded that the STO-3G basis-set is insufficient to describe polarization effects due to the lack of polarization functions.

D. Dependence of the Polarizability on the Conformation of Carbon and BN Tubes. In Table 3, results from calculations of a number of selected nanotubes are displayed. It is seen that the polarizability perpendicular and along the tube are lowered when going from a C-NT to a BN-NT with the same geometry and number of atoms. This is found both for armchair and zigzag

TABLE 3: Static Polarizabilities of Selected Nanotubes Calculated from the IM (in au)

nanotube[a]	$\bar{\alpha}$	λ	$\alpha_{\parallel}$	$\alpha_{\perp}$
$[5,5]C^{100}$	991.2	414.7	1267.7	854.4
$[5,5]BN^{100}$	823.7	338.2	1049.1	710.9
$[10,0]BN^{100}$	825.6	220.6	972.6	752.1
$[9,0]BN^{90}$	744.3	248.0	909.6	661.6
$[9,0]C^{90}$	877.9	288.9	1070.6	781.6

[a] Superscript indicates number of atoms.

configurations. The relative difference in polarizability per unit is on the same order of magnitude as that found between benzene and borazine in Table 1. As discussed above, this difference in the polarizability is due to the more delocalized π-electrons in the benzene-like structure of the C-NTs than in the BN-NTs. It is also seen from Table 3 that the anisotropy of the polarizability is larger in the C-NTs than in the BN-NTs. Furthermore, the anisotropy of all the tubes represented in Table 3 is a factor 10−20 larger than for the benzene and borazine molecules in Table 1, which more or less corresponds to the difference in number of atoms even if an additive model cannot be adopted.

The geometry of the tube also plays an importent role for the polarizability. In Table 3, the polarizability of an armchair and a zigzag conformation, both with 100 boron and nitrogen atoms, are compared. For the zigzag nanotube, the polarizability along the tube is lower, and the component perpendicular to the tube is higher than the polarizability for the corresponding armchair tube. However, the mean polarizability is almost the same for the two conformations. This trend was also found for the polarizability[11,15,18] and for the mean static hyperpolarizability[15−17] of C-NTs. In addition, the anisotropy for the zigzag configuration is lower than that for the armchair configuration. Consequently, the intramolecular geometry has great influence on the molecular polarizability components but not on the mean polarizability. In contrast to the studies of the dependence of the band gap of carbon and BN nanotubes on the geometry, where large dependencies were found for carbon tubes but not for BN tubes,[67] we find a similar geometry dependence for the polarizability of the two types of tubes.

E. Frequency Dependence of the Polarizability Tensor of BN Tubes. In Figure 3, we present the dynamic polarizability calculated with the IM for two [6,6]-BN-NTs with 120 B and N atoms. One tube has hydrogens attached at the ends, and the other contains only B and N atoms. For the polarizability along the tube, the increase of the polarizability arising from the frequency dependence is about 7%, and for the polarizability perpendicular to the tube, the increase is about 3.0%. As for the carbon nanotubes,[18] we find that the frequency dependence along the tube is larger than that perpendicular to the tube, which results in an anisotropy which is somewhat more frequency-dependent than the mean polarizability. In general, however, the frequency dependence is relatively modest.

V. Conclusion

We have used an interaction model to calculate both static and frequency-dependent polarizability tensors for C_{60}, C-NTs, and BN-NTs. Furthermore, we have performed quantum mechanical calculations of the polarizability components of the smallest BN nanotubes. We find excellent agreement between the most accurate SCF calculations available in the literature, the IM results and experiments of the polarizability of C_{60}. Thus, the IM model provides a straightforward way of performing calculations of this kind when dealing with large systems. Also, good agreement is found in the trends predicted by SCF and IM when the number of atoms increases for the nanotubes. This is found both for increasing the length and the diameter of the nanotube. We find that adding hydrogen atoms to the end of a BN tube leads to a small increase of the polarizability. We also find that the C-NTs have larger polarizability components than the corresponding BN-NTs with the same geometry and number of atoms. The geometry affects the individual polarizability tensor components, whereas the mean polarizability is almost unaffected. Finally, it was found that the frequency dependence of the polarizability is relatively small.

Acknowledgment. L. J. gratefully acknowledges The Danish Research Training Council for financial support. K.V.M. thanks Statens Naturvidenskabelige Forskningsråd (SNF) and Statens Teknisk-Videnskabelige Forskningsråd (STVF) for support.

References and Notes

(1) Karna, S. P. *J. Phys. Chem. A* **2000**, *104*, 4671−4673.
(2) Shelton, D. P.; Rice, J. E. *Chem. Rev.* **1994**, *94*, 3−29.
(3) Kanis, D. R.; Ratner, M. A.; Marks, T. J. *Chem. Rev.* **1994**, *94*, 195−242.
(4) Bishop, D. M. *Adv. Quantum Chem.* **1994**, *25*, 1−45.
(5) Luo, Y.; Ågren, H.; Jørgensen, P.; Mikkelsen, K. V. *Adv. Quantum Chem.* **1995**, *26*, 165−237.
(6) Ajayan, P. M. *Chem. Rev.* **1999**, *99*, 1787−1799.
(7) Terrones, M.; Hsu, W. K.; Kroto, H. W.; Walton, D. R. M. *Top. Curr. Chem.* **1999**, *199*, 189−234.
(8) Iijima, S. *Nature* **1991**, *354*, 56−58.
(9) Iijima, S.; Ichihashi, T. *Nature* **1993**, *363*, 603−605.
(10) Bethune, D. S.; Kiang, C. H.; deVries, M. S.; Gorman, G.; Savoy, R.; Vazquez, J.; Beyers, R. *Nature* **1993**, *363*, 605−607.
(11) Benedict, L. X.; Louie, S. G.; Cohen, M. L. *Phys. Rev. B* **1995**, *52*, 8541−8549.
(12) Xie, R.-H.; Jiang, J. *Appl. Phys. Lett.* **1997**, *71*, 1029−1031.
(13) Xie, R.-H. *J. Chem. Phys.* **1998**, *108*, 3626−3629.
(14) Margulis, Vl. A.; Sizikova, T. A. *Phys. A* **1998**, *245*, 173−189.
(15) Wan, X.; Dong, J.; Xing, D. Y. *Phys. Rev. B* **1998**, *58*, 6756−6759.
(16) Jiang, J.; Dong, J.; Wan, X.; Xing, D. Y. *J. Phys. B: At. Mol. Opt. Phys.* **1998**, *31*, 3079.
(17) Jiang, J.; Dong, J.; Xing, D. Y. *Phys. Rev. B* **1999**, *59*, 9838−9841.
(18) Jensen, L.; Schmidt, O. H.; Mikkelsen, K. V.; Åstrand, P.-O. *J. Phys. Chem. B* **2000**, *104*, 10462−10466.
(19) Lü, W.; Dong, J.; Li, Z.-Y. *Phys. Rev. B* **2000**, *63*, 033401−1−4.
(20) Liu, X.; Si, J.; Chang, B.; Xu, G.; Yang, Q.; Pan, Z.; Xi, S.; Ye, P. *Appl. Phys. Lett.* **1999**, *74*, 164−166.
(21) Wang, S.; Huang, W.; Yang, H.; Gong, Q.; Shi, Z.; Zhou, X.; Qiang, D.; Gu, Z. *Chem. Phys. Lett.* **2000**, *320*, 411−414.
(22) Oh, D.-H.; Park, J. M.; Kin, K. S. *Phys. Rev. B* **2000**, *62*, 1600−1603.
(23) Wang, N.; Tang, Z. K.; Li, G. D.; Chen. J. S. *Nature* **2000**, 408, 50.
(24) Fowler, P. W.; Lazzeretti, P.; Zanasi, R. *Chem. Phys. Lett.* **1990**, *165*, 79−86.
(25) Talapatra, G. B.; Manickam, N.; Samoc, M.; Orczyk, M. E.; Karna, S. P.; Prasad, P. N. *J. Phys. Chem.* **1992**, *96*, 5206−5208.
(26) Weiss, H.; Ahlrichs, R.; Häser, M. *J. Chem. Phys.* **1993**, *99*, 1262−1270.
(27) Shanker, B.; Applequist, J. *J. Phys. Chem.* **1994**, *98*, 6486.
(28) van Gisbergen, S. J. A.; Snijders, J. G.; Baerends, E. J. *Phys. Rev. Lett.* **1997**, *78*, 3097−3100.
(29) Jonsson, D.; Norman, P.; Ruud, K.; Ågreen, H.; Helgaker, T. *J. Chem. Phys.* **1998**, *109*, 572.
(30) Ruud, K.; Jonsson, D.; Taylor, P. R. *J. Chem. Phys.* **2001**, *114*, 4331−4332.
(31) Ruiz, A.; Bretón, J.; Llorente, J. M. G. *J. Chem. Phys.* **2001**, *114*, 1272−1277.
(32) Blau, W. J.; Byrne, H. J.; Cardin, D. J.; Dennis, T. J.; Hare, J. P.; Kroto, H. W.; Taylor, R.; Walton, D. R. M. *Phys. Rev. Lett.* **1991**, *67*, 1423−1425.
(33) Hebard, A. F.; Haddon, R. C.; Fleming, R. M.; Kortan, A. R. *Appl. Phys. Lett.* **1991**, *59*, 2109−2111.
(34) Hansen, P. L.; Fallon, P. J.; Krätschmer, W. *Chem. Phys. Lett.* **1991**, *181*, 367−372.
(35) Wang, Y.; Cheng, L.-T. *J. Phys. Chem.* **1992**, *96*, 1530−1532.
(36) Kafafi, Z. H.; Lindle, J. R.; Pong, R. G. S.; Bartoli, F. J.; Lingg, L. J.; Milliken, J. *Chem. Phys. Lett.* **1992**, *188*, 492−496.

(37) Ren, S. L.; Wang, K. A.; Zhou, P.; Wang, Y.; Rao, A. M.; Meier, M. S.; Selegue, J. P.; Eklund, P. C. *Appl. Phys. Lett.* **1992**, *61*, 124−126.

(38) Eklund, P. C.; Rao, A. M.; Wang, Y.; Zhou, P.; Wang, K. A.; Holden, J. M.; Dresselhaus, M. S.; Dresselhaus, G. *Thin Solid Films* **1995**, *257*, 211−232.

(39) Antoine, R.; Dugourd, Ph.; Rayane, D.; Benichou, E.; Broyer, M.; Chandezon, F.; Guet, C. *J. Chem. Phys.* **1999**, *110*, 9771−9772.

(40) Ballard, A.; Bonin, K.; Louderback, J. *J. Chem. Phys.* **2000**, *113*, 5732.

(41) Stephan, O.; Ajayan, P. M.; Colliex, C.; Redlich, Ph.; Lambert, J. M.; Bernier, P.; Lefin, P. *Science* **1994**, *266*, 1683−1685.

(42) Weng-Sieh, Z.; Cherrey, K.; Chopra, N. G.; Blase, X.; Miyamoto, Y.; Rubio, A.; Cohen, M. L.; Louie, S. G.; Zettl, A.; Gronsky, R. *Phys. Rev. B* **1995**, *51*, 11229−11232.

(43) Terrones, M.; Benito, A. M.; Manteca-Diego, C.; Hsu, W. K.; Osman, O. I.; Hare, J. P.; Reid, D. G.; Terrones, H.; Cheetham, A. K.; Prassides, K.; Kroto, H. W.; Walton, D. R. M. *Chem. Phys. Lett.* **1996**, *257*, 576−582.

(44) Redlich, Ph.; Loeffler, J.; Ajayan, P. M.; Bill, J.; Aldinger, F.; Rühle, M. *Chem. Phys. Lett.* **1996**, *260*, 465−470.

(45) Zhang, Y.; Gu, H.; Suenaga, K.; Iijima, S. *Chem. Phys. Lett.* **1997**, *279*, 264−269.

(46) Sen, R.; Satishkumar, B. C.; Govindaraj, A.; Harikumar, K. R.; Raina, G.; Zhang, J.-P.; Rao, C. N. R. *Chem. Phys. Lett.* **1998**, *287*, 671−676.

(47) Golberg, D.; Bando, Y.; Han, W.; Kurashima, K.; Sato, T. *Chem. Phys. Lett.* **1999**, *308*, 337−342.

(48) Suenaga, K.; Johansson, M. P.; Hellgren, N.; Broitman, E.; Wallenberg, L. R.; Colliex, C.; Sundgren, J.-E.; Hultman, L. *Chem. Phys. Lett.* **1999**, *300*, 695−700.

(49) Han, W.; Bando, Y.; Kurashima, K.; Sato, T. *Chem. Phys. Lett.* **1999**, *299*, 368−373.

(50) Hamilton, E. J. M.; Dolan, S. E.; Mann, C. M.; Colijn, H. O.; McDonald, C. A.; Shore, S. G. *Science* **1993**, *260*, 659−661.

(51) Chopra, N. G.; Luyken, R. J.; Cherrey, K.; Crespi, V. H.; Cohen, M. L.; Louie, S. G.; Zetti, A. *Science* **1995**, *269*, 966−967.

(52) Golberg, D.; Bando, Y.; Eremets, M.; Takemura, K.; Kurashima, K.; Yusa, H. *Appl. Phys. Lett.* **1996**, *69*, 2045−2047.

(53) Terrones, M.; Hsu, W. K.; Terrones, H.; Zhang, J. P.; Ramos, S.; Hare, J. P.; Castillo, R.; Prassides, K.; Cheetman, A. K.; Kroto, H. W.; Walton, D. R. M. *Chem. Phys. Lett.* **1996**, *259*, 568−573.

(54) Loiseau, A.; Willaime, F.; Demoncy, N.; Hug, G.; Pascard, H. *Phys. Rev. Lett.* **1996**, *76*, 4737−4740.

(55) Loiseau, A.; Willaime, F.; Demoncy, N.; Schramchenko, N.; Hug, G.; Colliex, C.; Pascard, H. *Carbon* **1998**, *36*, 743−752.

(56) Sen, R.; Satishkumar, B. C.; Govindaraj, A.; Hariku mar, K. R.; Renganathan, M. K.; Rao, C. N. R. *J. Mater. Chem.* 1997, *7*, 2335−2337.

(57) Chen, Y.; Chadderton, L. T.; Gerald, J. F.; Williams, J. S. *Appl. Phys. Lett.* **1999**, *74*, 2960−2962.

(58) Shimizu, Y.; Moriyoshi, Y.; Tanaka, H.; Komatsu, S. *Appl. Phys. Lett.* **1999**, *75*, 929−931.

(59) Cumings, J.; Zettl, A. *Chem. Phys. Lett.* **2000**, *316*, 211−216.

(60) Chen, Y.; Gerald, J. F.; Williams, J. S.; Bulcock, S. *Chem. Phys. Lett.* **1999**, *299*, 260−264.

(61) Terauchi, M.; Tanaka, M.; Suzuki, K.; Ogino, A.; Kimura, K. *Chem. Phys. Lett.* **2000**, *324*, 359−364.

(62) Saito, Y.; Maida, M. *J. Phys. Chem. A* **1999**, *103*, 1291−1293.

(63) Yi, J.-Y.; Bernholc, J. *Phys. Rev. B* **1993**, *47*, 1708−1711.

(64) Rubio, A.; Corkill, J. L.; Cohen, M. L. *Phys. Rev. B* **1994**. *49*, 5081−5084.

(65) Miyamoto, Y.; Rubio, A.; Cohen, M. L.; Louie, S. G. *Phys. Rev. B* **1994**, *50*, 4976−4979.

(66) Miyamoto, Y.; Rubio, A.; Louie, S. G.; Cohen, M. L. *Phys. Rev. B* **1994**, *50*, 18360−18366.

(67) Blase, X.; Rubio, A.; Louie, S. G.; Cohen, M. L. *Europhys. Lett.* **1994**, *28*, 335−340.

(68) Blase, X.; Charlier, J.-C.; De Vita, A.; Car, R. *Appl. Phys. Lett.* **1997**, *70*, 197−199.

(69) Wang, B.-C.; Tsai, M.-H.; Chou, Y.-M. *Synth. Met.* **1997**, *86*, 2379−2380.

(70) Menon, M.; Srivastava, D. *Chem. Phys. Lett.* **1999**, *307*, 407−412.

(71) Carroll, D. L.; Redlich, P.; Ajayan, P. M.; Curran, S.; Roth, S.; Rühle, M. *Carbon* **1998**, *36*, 753−756.

(72) Blase, X.; Charlier, J.-C.; De Vita, A.; Car, R. *Appl. Phys. A* **1999**, *68*, 293−300.

(73) Fowler, P. W.; Rogers, K. M.; Seifert, G.; Terrones, M.; Terrones, H. *Chem. Phys. Lett.* **1999**, *299*, 359−367.

(74) Pokropivny, V. V.; Skorokhod, V. V.; Oleinik, G. S.; Kurdyumov, A. V.; Bartnitskaya, T. S.; Pokropivny, A. V.; Sisonyuk, A. G.; Scheichenko, D. M. *J. Solid State Chem.* **2000**, *154*, 214−222.

(75) Hirano, T.; Oku, T.; Suganuma, K. *Diamond and Related Materials* **2000**, *9*, 625−628.

(76) Erkoç, Ş. *J. Mol. Struc. (THEOCHEM)* **2001**, *542*, 89−93.

(77) Xie, R. H. *Chem. Phys. Lett.* **1999**, *310*, 379−384.

(78) Dong, J.; Jiang, J.; Yu, J.; Wang, Z. D.; Xing, D. Y. *Phys. Rev. B* **1995**, *52*, 9066−9070.

(79) Xu, Q.; Dong, J.; Jiang, J.; Xing, D. Y. *J. Phys. B: At. Mol. Opt. Phys.* **1996**, *29*, 1563−1568.

(80) Jensen, L.; Åstrand, P.-O.; Sylvester-Hvid, K. O.; Mikkelsen, K. V. *J. Phys. Chem. A* **2000**, *104*, 1563.

(81) Jensen, L.; Osted, A.; Kongsted, J.; Åstrand, P.-O.; Mikkelsen, K. V. *J. Chem. Phys.* **2001**, submitted.

(82) Applequist, J.; Carl, J. R.; Fung, K.-F. *J. Am. Chem. Soc.* **1972**, *94*, 2952.

(83) Frisch, M. J.; Trucks, G. W.; Schlegel, H. B.; Scuseria, G. E.; Robb, M. A.; Cheeseman, J. R.; Zakrzewski, V. G.; Montgomery, J. A., Jr.; Stratmann, R. E.; Burant, J. C.; Dapprich, S.; Millam, J. M.; Daniels, A. D.; Kudin, K. N.; Strain, M. C.; Farkas, O.; Tomasi, J.; Barone, V.; Cossi, M.; Cammi, R.; Mennucci, B.; Pomelli, C.; Adamo, C.; Clifford, S.; Ochterski, J.; Petersson, G. A.; Ayala, P. Y.; Cui, Q.; Morokuma, K.; Malick, D. K.; Rabuck, A. D.; Raghavachari, K.; Foresman, J. B.; Cioslowski, J.; Ortiz, J. V.; Stefanov, B. B.; Liu, G.; Liashenko, A.; Piskorz, P.; Komaromi, I.; Gomperts, R.; Martin, R. L.; Fox, D. J.; Keith, T.; Al-Laham, M. A.; Peng, C. Y.; Nanayakkara, A.; Gonzalez, C.; Challacombe, M.; Gill, P. M. W.; Johnson, B. G.; Chen, W.; Wong, M. W.; Andres, J. L.; Head-Gordon, M.; Replogle, E. S.; Pople, J. A. *Gaussian 98*, revision A.7; Gaussian, Inc.: Pittsburgh, PA, 1998.

(84) *SPARTAN 4.1.2*; Wavefunction: Irvine, CA, 1996.

(85) Kwon, Y.-K (http://www.pa.msu.edu/ykkwon/nanotubes/coordinates.html, accessed 1998).

(86) Frisch, M. J.; Trucks, G. W.; Schlegel, H. B.; Gill, P. M. W.; Johnson, B. G.; Robb, M. A.; Cheeseman, J. R.; Keith, T.; Petersson, G. A.; Montgomery, J. A.; Raghavachari, K.; Al-Laham, M. A.; Zakrzewski, V. G.; Ortiz, J. V.; Foresman, J. B.; Cioslowski, J.; Stefanov, B. B.; Nanayakkara, A.; Challacombe, M.; Peng, C. Y.; Ayala, P. Y.; Chen, W.; Wong, M. W.; Andres, J. L.; Replogle, E. S.; Gomperts, R.; Martin, R. L.; Fox, D. J.; Binkley, J. S.; Defrees, D. J.; Baker, J.; Stewart, J. P.; Head-Gordon, M.; Gonzalez, C.; Pople, J. A. *Gaussian 94*, revision B.3; Gaussian, Inc.: Pittsburgh, PA, 1995.

(87) Russell, A. J.; Spackman, M. A. *Mol. Phys.* **1996**, *88*, 1109−1136.

(88) Jensen, L.; Åstrand, P.-O.; Mikkelsen, K. V. *Int. J. Quant. Chem.* **2001**, *84*, 513−522.

(89) Lide, D. R. *Handbook of Chemistry and Physics*, 73rd ed.; CRC Press: London, 1992−1993.

(90) Lazzeretti, P.; Tossel, J. A. *J. Mol. Struc. (THEOCHEM)* **1991**, *236*, 403−410.

(91) Helgaker, T.; Jensen, H. J. Aa.; Jørgensen, P.; Olsen, J.; Ruud, K.; Ågren, H.; Andersen, T.; Bak, K. L.; Bakken, V.; Christiansen, O.; Dahle, P.; Dalskov, E. K.; Enevoldsen, T.; Fernandez, B.; Heiberg, H.; Hettema, H.; Jonsson, D.; Kirpekar, S.; Kobayashi, R.; Koch, H.; Mikkelsen, K. V.; Norman, P.; Packer, M. J.; Saue, T.; Taylor, P. R.; Vahtras, O. *Dalton* Release 1.0; 1997. http://www.kjemi.uio.no/software/dalton/